Preparation and Photophysical Characterization of a Y-Zeolite-Entrapped $Ru(bpy)_2(pypz)^{2+}$ Complex

Witold S. Szulbinski and James R. Kincaid*

Department of Chemistry, Marquette University, Milwaukee, Wisconsin 53201-1881

Received August 25, 1997

In this work, the generation of a new Y-zeolite-entrapped $Ru(bpy)_2(pypz)^{2+}$ complex is reported, where bpy = 2,2′-bipyridine and pypz = 2-(2-pyridyl)pyrazine. The integrity of the sample was documented by UV−visible, emission, resonance Raman (RR), and time-resolved resonance Raman (TR^3) spectroscopic data, as well as lifetime measurements. The Raman spectrum for the ground-state $Z-Ru(bpy)_2(pypz)^{2+}$ intrazeolitic complex, with laser excitation at λ_{ex} = 413.1 and 488.0 nm, closely matched that obtained for the free $[Ru(byp)_2(pypz)]Cl_2$ complex, with some bands exhibiting slight frequency shifts of 2−5 cm^{-1}. This finding indicates that the structure of the Ru^{2+} complex does not change substantially upon entrapment in the Y-zeolite supercages. On the other hand, the emission spectroscopic investigation revealed a 16 nm blue shift of the $Z-Ru(bpy)_2(pypz)^{2+}$ phosphorescence, relative to that of the free $[Ru(bpy)_2(pypz)]Cl_2$ complex, and the lifetime measurements revealed a 210 ns increase of the triplet excited-state (^{3}MLCT) lifetime. These data suggest perturbation of the $Ru(byp)_2(pypz)^{2+}$ complex electronic structure, presumably induced by interaction of the peripheral N heteroatom with the zeolite framework. Temperature-dependent lifetime measurements indicated that decay via the thermally populated, so-called, "fourth MLCT state" (4th-MLCT) was dominant both for the $Ru(bpy)_2(pypz)^{2+}$ complex in solution and for the complex entrapped within the zeolite supercages.

Introduction

Recently, a method for generation of structurally diverse zeolite-entrapped Ru^{2+} complexes has been developed in our laboratory, and the photophysical properties of several of those have now been carefully documented.[1] Moreover, it also has been demonstrated that those intrazeolitic complexes which possess ligands bearing peripheral nitrogen atoms, such as $Z-Ru(bpy)_2(bpz)^{2+}$ (where bpy is 2,2′-bipyridine and bpz is 2,2′-bipyrazine), are capable of coordinating another molecule of a Ru^{2+} amine complex in the Y-zeolite adjacent cages.[2] As is discussed elsewhere,[3] this approach may provide a route for the construction of highly efficient, intrazeolitic photocatalytic organized assemblies, in which components are arranged both spatially and in terms of reactivity.

With this in mind, we present here a study of a new zeolite-entrapped $Z-Ru(bpy)_2(pypz)^{2+}$ complex, where pypz is 2-(2-pyridyl)pyrazine as shown in Figure 1. The photochemical properties of the sample are considered with respect to those of the $Ru(bpy)_2(pypz)^{2+}$ free complex and compared to those of the $Z-Ru(bpy)_2(bpz)^{2+}$ and $Z-Ru(bpz)_3{}^{2+}$ intrazeolitic analogues. The results document a significant influence of the zeolite framework on the excited-state energy of the $Ru(bpy)_2(pypz)^{2+}$ complex.

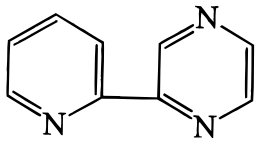

pypz

Figure 1. Schematic representation of the pypz ligand.

Experimental Section

A. Materials. Samples of Y-zeolite, $RuCl_3$, 2,2′-bpy, 2-bromopyridine, 2-choloropyrazine, NaH, *tert*-butyl alcohol, triphenylphosphine, dimethoxyethane, and all solvents were purchased from Aldrich Chemical Co. The 2,2′-bpy was sublimed and pypz was purified by column chromatography prior to use. The samples of the $Ru(NH_3)_6Cl_3$ salt were obtained from Alfa Inorganics.

B. Preparation of Compounds. 1. Synthesis of 2-(2-Pyridyl)-pyrazine (pypz). The pypz ligand was obtained by reductive condensation of 2-bromopyridine with 2-choloropyrazine catalyzed by the nickel complex reductive agent (NiCRA; NaH−*t*-BuONa−$Ni(OAc)_2$).[4] Since the procedure is a modified version of that reported elsewhere,[4,5a] we describe below the synthesis of pypz in detail. This modification regards generation of NiCRA catalyst using a mixture of triphenylphosphine and 2,2′-bipyridine, replacement of 2-chloropyridine by 2-bromopyridine, and separation of the pure pypz from the crude product (a

* To whom correspondence should be addressed.

(1) (a) Maruszewski, K.; Strommen, D. P.; Handrich, K.; Kincaid, J. R. *Inorg. Chem.* **1991**, *30*, 4579−4582. (b) Maruszewski, K.; Strommen, D. P.; Kincaid, J. R. *J. Am. Chem. Soc.* **1993**, *115*, 8345−8350. (c) Maruszewski, K.; Kincaid, J. R. *Inorg. Chem.* **1995**, *34*, 2002−2006.

(2) (a) Sykora, M.; Maruszewski, K.; Treffert-Ziemelis, S. M.; Kincaid, J. R. *J. Am. Chem. Soc.*, submitted. (b) Sykora, M.; Kincaid, J. R. *Nature* **1997**, *387*, 162−164.

(3) (a) Dutta, P. K.; Ledney, M. *Progress in Inorganic Chemistry*; J. Wiley & Sons: Inc.: New York, 1997; Vol. 44, pp 209−271. (b) Borja, M.; Dutta, P. K. *Nature* **1993**, *362*, 43−45. (c) Incavo, J. A.; Dutta, P. K. *J. Phys. Chem.* **1990**, *94*, 3075. (d) Bedioui, F. *Coord. Chem. Rev.* **1995**, *144*, 39−68. (e) Kalyanasundaram, K. *Photochemistry in Microheterogeneous Systems*; Academic Press: Orlando, FL, 1987. (f) Ramamurthy, V. *Photochemistry in Organized and Constrained Media*; VCH: New York, 1991.

(4) (a) Vanderesse, R.; Lourak, M.; Fort, Y.; Caubere, P. *Tetrahedron Lett.* **1986**, *27*, 5483−5486. (b) Brunet, J.-J.; Besozzi, D.; Courtois, A.; Caubere, O. *J. Am. Chem. Soc.* **1982**, *104*, 7130−35.

(5) (a) Danzer, G. D.; Golus, J. A.; Kincaid, J. R. *J. Am. Chem. Soc.* **1993**, *115*, 8643−8648. (b) McClanahan, S. F.; Dallinger, R. F.; Holler, F. J.; Kincaid, J. R. *J. Am. Chem. Soc.* **1985**, *107*, 4853.

S0020-1669(97)01088-4 CCC: $15.00
Published on Web 02/10/1998

mixture of PPh_3, bpy, bpz, and pypz) using a Soxhlet extraction procedure and a modified chromatographic method.

The NiCRA was obtained from 1.2 g (10 mmol) of anhydrous nickel acetate, 10.48 g (40 mmol) of triphenylphosphine (PPh_3), 0.5 g (3.2 mmol) of bpy, and 1.44 g (60 mmol) of NaH mixed together in 30 mL of dry dimethoxyethane (DME). After 15 min of stirring at 60−65 °C, 1.48 g (20 mmol, 2 mL) of *tert*-butyl alcohol (*t*-BuOH) in 10 mL of DME was added to the reaction mixture in a dropwise fashion. The stirring was continued for the next 2 h at 60 °C. In that time, the color of the NiCRA catalyst changed to brown-red. Then, 0.45 mL (5 mmol) of 2-chloropyrazine and 0.5 mL (5 mmol) of 2-bromopyridine diluted in 10 mL of DME were added in a dropwise fashion. The reaction mixture was left for the next 5 h with stirring at 60 °C and under dry nitrogen. Then, after the mixture was cooled to 0 °C, 50 mL of 75% ethanol was added, in a dropwise fashion, to decompose unreacted NaH. Subsequently, the reaction mixture was evaporated to dryness using a rotating evaporator. The residual brown-black solid was extracted with 400 mL of ethyl ether using a Soxhlet apparatus to wash out the mixture of four products: bpy, bpz, pypz, and PPh_3. After condensation of the Et_2O extract to around 15 mL using a rotating evaporator [*caution*!], the remaining brown-yellow oil was chromatographed on a silica gel column using 1:1 ethyl acetate/hexane as the eluent. The pypz was obtained in the third fraction (the PPh_3 was first and the bpy was second). The purity of the pypz sample was confirmed by GC/MS analysis, which exhibited the expected molecular ion peak for $pypz^+$ at $m/z = 157$. Yield: 95 mg (12%).

2. Synthesis of $[Ru(bpy)_2]Cl_2$ and $[Ru(bpy)_2(pypz)]Cl_2$. The $[Ru(bpy)_2]Cl_2$ complex was obtained from $RuCl_3 \cdot 3H_2O$ and the stoichiometric amount of 2,2′-bpy in dry DMF, in the presence of LiCl, as described elsewhere.[6] The product was recrystallized from hot water.

The $[Ru(bpy)_2(pypz)]Cl_2$ complex was generated from $[Ru(bpy)_2]Cl_2$ and the stoichiometric amount of pypz in EtOH.[5] The crude product was precipitated as the PF_6^- salt, and then purified by metathesis[7] with Et_4NCl in acetone to obtain its Cl^- salt.

Generation of $Z-Ru(bpy)_2^{2+}$ and $Z-Ru(bpy)_2(pypz)^{2+}$ Samples. To obtain two samples of the ion-exchanged $Z-Ru^{3+}$ zeolite with a load of one Ru^{3+} cation per 60 supercages (1:60) and another having one Ru^{3+} cation per 15 supercages (1:15), 5 and 20 mg of $Ru(NH_3)_6Cl_3$, respectively, were mixed with 2 g of the Y-zeolite (calcinated at 500 °C, washed with 20% aqueous NaCl, and then with deionized (DI) water).[1a] It was assumed that 2 g of the Y-zeolite contained 5.556×10^{20} supercages.[8] During this ion-exchange operation, the solution was stirred vigorously and kept in the dark at 4 °C, for 24 h. Then, the zeolite was filtered off, washed with DI water, and air-dried. After that, 1.0 g of $Z-Ru^{3+}$ was mixed in a high-vacuum reaction vessel (∼2.5 cm × 12.5 cm) with 30−50 mg of 2,2′-bpy dissolved in ethanol and kept overnight at 4 °C. subsequently, the ethanol was evaporated under a stream of dry nitrogen. The solid mixture was evacuated to 10^{-3} Torr and held at that pressure for the next 5 h. Then, the vessel's stopcock was closed and the powder was heated at 85−90 °C for 20 h, during which the sample changed color to pink-brown. It is important to note that if the mixture was heated for period of time shorter than 12 h, the zeolite was mainly loaded with $Ru(bpy)X_4^{2+}$ complex (where $X = NH_3$ or H_2O)[9] as evidenced by DR and the UV−visible spectrum of its HCl extract. The $Ru(bpy)^{2+}$ species exhibits absorption at $\lambda_{max} = 367$ and 523 nm,[10] whereas the $Ru(bpy)_2^{2+}$ complex absorbs at 350 and 495 nm,[11] so they can be easily recognized one from another. After cooling, the crude product was extracted with ethanol in a Soxhlet apparatus. To facilitate desorption of the unreacted 2,2′-bpy and any residual $Ru(bpy)X_4^{2+}$ from the zeolite, 5−10 g of solid NaCl was placed in the Soxhlet thimble. The extraction was conducted until the total amount of the solid NaCl had been washed out from the Soxhlet thimble, and the UV spectrum of the ethanolic extract did not show absorption typical of the ligand (at 254 nm). This operation required approximately 5 days. Subsequently, the zeolite was washed with DI water (500 mL), to remove from the zeolitic samples any residual NaCl, and then dried in air. The integrity of the $Z-Ru(bpy)_2^{2+}$ sample was confirmed, as described previously,[1a] by emission, RR, and electronic absorption spectra of its HCl extract. The $Z-Ru(bpy)_2^{2+}$ samples were contaminated with the $Z-Ru(bpy)_3^{2+}$ species by less than 0.1% as evidenced by comparing their luminescence at 610 nm to that of the sample after spiking with a portion (5 wt %) of $Z-Ru(bpy)_3^{2+}$ complex with the same loads.

In the next step, the $Z-Ru(bpy)_2^{2+}$ zeolite was thoroughly mixed with 2 mL of an ethanolic solution containing an appropriate amount of the pypz ligand (140 mg for the load of 1:15 and 80 mg for the load of 1:60). Then, the reaction mixture was kept at 20 °C for 24 h. After evaporation of the ethanol, the sample was evacuated at 10^{-3} Torr for 5 h and then heated at 200 °C for 3 days. In that time, the zeolite changed color from pink to yellow. Subsequently, the crude product was extracted with ethanol in a Soxhlet apparatus with 5 g of solid NaCl in the Soxhlet thimble in order to remove the excess of unreacted pypz. This operation was conducted for 5−7 days, until all the ligand was washed out from the zeolite, as evidenced by UV−visible spectroscopy of the ethanolic extract. Because the emission spectrum of the sample exhibited luminescence of unidentified impurities (which probably came from products of pypz decomposition or polymerization) at 421, 510, and 825 nm, the $Z-Ru(bpy)_2(pypz)^{2+}$ sample, after the Soxhlet extraction, was stirred in boiling 20% NaCl for 3 days. This operation was repeated three times until no emission of the impurities was observed. Finally, the zeolite was thoroughly washed with hot DI water (500 mL) and dried under nitrogen at 110 °C.

C. Spectroscopic Measurements. 1. UV−visible absorption spectra were obtained with a Hewlett-Packard Model 8452A diode array spectrometer.

2. Resonance Raman (RR) and time-resolved resonance Raman (TR^3) spectra were acquired using a Spex Model 1269 spectrometer equipped with a Princeton Instruments ICCD-576 UV-enhanced detector, FG-100 pulse generator, and 356 or 413 nm notch filters (Kaiser Optical Systems, Ann Arbor, MI); a Spex Model 1877 spectrometer equipped with a Tracor Northern rapid-scan spectrometer, Model TN-6500, and diode array detector, Model TN-6100; a conventional Raman spectrometer based on a Spex Model 1403 double monochromator equipped with a Spex Model DM1B controller and a Hamamatsu R928 PMT. The excitation sources used were the 350.9, 406.7, and 413.1 nm laser lines from a Coherent Model Innova 100-K3 Kr^+ ion laser; the 457.9 and 488.0 nm laser lines from a Spectra-Physics Ar^+ ion laser, Model 2025-05; or 441.6 nm laser line from a Liconix Model 4240 He−Cd ion laser. All Raman spectra of the $[Ru(bpy)_2(pypz)]Cl_2$ complex in water and the $Z-Ru(bpy)_2(pypz)^{2+}$ sample, suspended in DI water, were obtained in rotating NMR tubes (5 mm i.d.) to avoid localized heating by the laser beam. The scattered light was collected with 135° backscattering geometry and a conventional two-lens collection system. Before the measurements, the solid samples were degassed at 10^{-4} Torr for 3 h, whereas the liquid samples (prepared in DI water or propylene carbonate, PC) were degassed by triple freeze−pump−thaw cycles, directly in the NMR tubes, which were then sealed.

3. Emission Spectra. The spectroscopic apparatus was the same as for the Raman measurements (Spex Model 1403). The laser excitation was focused onto spun NMR tubes containing the samples, with a laser power of 10−20 mW at the sample. Spectra were recorded with 40 cm^{-1} increments. The emission spectra are not corrected for the instrument response.

4. Lifetime Measurements. The samples for the measurements were degassed as described before. The third harmonic (354.7 nm; 10−15 ns pulse width) of a Quanta-Ray (Spectra-Physics) Model GCR-11 or DCR-3 Nd^{3+}:YAG laser (operated at 20 Hz frequency) was used as the excitation source (the power at the sample was in all cases below 0.05 mJ/pulse). The light emitted from the sample in the spinning NMR tube was transferred through glass collecting and transferring lenses and a 580 nm cutoff filter to a Spex 340S spectrometer equipped with

(6) Sprintschnik, G.; Sprintschnik, H. W.; Krisch, P. P.; Whitten, D. G. *J. Am. Chem Soc.* **1977**, *99*, 4947−4954.
(7) Szulbinski, W. S.; Busch, D. H. *Inorg. Chim. Acta* **1995**, *234*, 143−148.
(8) Breck, D. W. *Zeolite Molecular Sieves*; John Wiley & Sons: New York, 1974; p 177.
(9) Szulbinski, W. S.; Kincaid, J. R. Unpublished results.
(10) Alvarez, V. E.; Allen, R. J.; Matsubura, T.; Ford, P. C. *J. Am. Chem. Soc.* **1976**, *96*, 7687.
(11) Bryant, G. M.; Fergusson, J. E.; Powell, H. K. *Aust. J. Chem.* **1971**, *24*, 257.

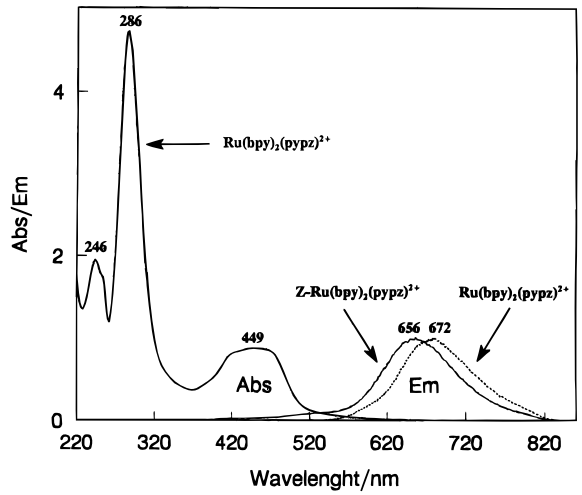

Figure 2. UV−visible absorption (Abs) and emission (Em) spectra, aquired with 441.6 nm excitation, for aqueous $[Ru(bpy)_2(pypz)]Cl_2$ (0.1 mM) at 20 °C. The emission spectrum of $Z-Ru(bpy)_2(pypz)^{2+}$ suspended in DI water, obtained with 350.9 nm excitation at 20 °C, is marked with a solid line.

an RCAC31034A-02 PMT with an applied voltage of 1800 V. The PMT output signal was directed to a LeCroy 9450A Dual 300 MHz oscilloscope. The emission was monitored at an appropriately chosen wavelength (at 655 nm for $Z-Ru(bpy)_2(pypz)^{2+}$ and 672 nm for $[Ru(bpy)_2(pypz)]Cl_2$). In all cases, 3000 scans of the emission decay curve were averaged and transferred to the computer. The curves were then fitted by a monoexponential model using facilities of the commercial software (PSI-Plot) based on the Marquardt−Levenberg algorithm.

For the temperature-dependent lifetime measurements, the samples were placed into a double-wall dewar cell of in-house design. Prior to the measurement the samples were thoroughly degassed by freeze−pump−thaw cycles (for the $Z-Ru(bpy)_2(pypz)^{2+}$ with the load of 60:1) or deaerated by bubbling Ar through the solution (for the PC solution of the $[Ru(bpy)_2(pypz)](PF_6)_2$ complex with a concentration $<10^{-5}$ M). During the experiments, the PC solution was continuously stirred by a magnetic stirrer and the zeolite sample was spun to prevent local overheating and possible decomposition of the compounds. The temperature of the sample was measured with 0.1 °C accuracy using a thermocouple inserted into the sample or placed, as close as possible, to the spinning tube with sample immersed in the cooling (heating) bath. For the low-temperature measurements, the samples were cooled by an EtOH/liquid-nitrogen mixture (−60 °C) and then allowed to slowly warm to room temperature. During this period (3−4 h), the lifetime measurements were acquired every 3−4 °C change in temperature. The temperature variation during the collection of the data (500 sweeps/25 s) was approximately 0.3−0.5 °C. The measurements at temperatures above 20 °C were taken with the same setup using boiling water as the heating fluid. After pouring it into the cell water jacket, the temperature increased immediately to ∼90 °C (a part of the thermal energy was consumed to warm the cell). Then it began to decrease (2−1 °C/min), however, too fast to perform the measurements. Thus, these kinetics started to be measurable from ∼75 °C, when the temperature change slowed appropriately (0.3−0.5 °C/30 s).

Results and Discussion

A. UV−Visible and Emission Data. 1. The $[Ru(bpy)_2(pypz)]Cl_2$ Complex. The absorption and emission spectra of the aqueous $[Ru(bpy)_2(pypz)]Cl_2$ complex (0.1 mM) is shown in Figure 2. The UV−Visible spectrum consists of three bands centered at 246, 286, and 449 nm. The broad electronic absorption envelope centered at $\lambda_{max} = 449$ nm is assigned to MLCT transitions,[12] whereas those bands at $\lambda_{max} = 286$ and 246 nm are due to $\pi \rightarrow \pi^*$ transitions within the ligands.[13] The absorption at 449 nm can be assigned to various electronic transitions between $d\pi(T_{2g})$ orbitals of the metal, and the π^* orbitals of the pypz and bpy ligands.[5] Inasmuch as the pypz π^* orbital is lower in energy than that of the bpy ligand,[13] it is expected that the absorption bands falling within the low-energy side of the envelope are ascribable to Ru → pypz transitions, while the higher energy bands are associated with Ru → bpy transitions.

The emission spectrum of an aqueous solution of the $[Ru(bpy)_2(pypz)]Cl_2$ complex (0.1 mM), obtained with 441.6 nm excitation, revealed phosphorescence at $\lambda_{em} = 672$ nm, as shown in Figure 2 with a dotted line. As was clarified above, the pypz π^* orbital is lower in energy than those of bpy ligands and the transition giving rise to the luminescence is most reasonably ascribed to $pypz^- \rightarrow Ru^{3+}$.

2. $Z-Ru(bpy)_2(pypz)^{2+}$. To confirm the identity of the $Z-Ru(bpy)_2(pypz)^{2+}$ complex, the zeolite framework was partially destroyed by treating with 0.2 N HCl, and after centrifugation and neutralization, its absorption spectrum closely matched that obtained for an authentic sample of the $Ru(bpy)_2(pypz)^{2+}$ complex.

The emission spectrum of the $Z-Ru(bpy)_2(pypz)^{2+}$ sample, suspended in degassed DI water, is shown in Figure 2. The $Z-Ru(bpy)_2(pypz)^{2+}$ zeolite exhibits strong phosphorescence centered at $\lambda_{em} = 656$ nm which is 16 nm blue shifted with respect to that of the free $Ru(bpy)_2(pypz)^{2+}$ complex in water. This shift can be explained by distortion of the Ru^{2+} complex ^{3}MLCT excited state, presumably due to electronic interaction of the peripheral N heteroatom in the pyrazine fragment with the zeolite framework (this unfavorable environment and this forced interaction result in an apparent increase in π and π^* orbitals). It is worth pointing out that in a previous study of $Z-Ru(bpy)_2(bpz)^{2+}$ (which possesses two peripheral N heteroatoms) a 31 nm blue shift was observed upon its entrapment in Y-zeolite;[1b] i.e., the complex of interest in this paper, having only one peripheral N heteroatom, exhibits a shift whose magnitude is only about half of that for the bpz-containing complex. For a solid $Z-Ru(bpy)_2(pypz)^{2+}$ sample which was kept under reduced pressure at 10^{-4} Torr, this emission is observed at $\lambda_{em} = 647$ nm. The additional blue shift of 9 nm is apparently attributable to an increased interaction with the zeolite framework brought about by partial dehydration.[3a,c]

B. Resonance Raman and TR^3 Data. The resonance Raman spectra of the $[Ru(bpy)_2(pypz)]Cl_2$ complex obtained with 488.0 and 413.1 nm excitation in the range of 1000−1650 cm^{-1} are shown in Figure 3, traces a and c. As discussed previously,[5a,14] they can be viewed as a composition of spectra associated with the two bpy symmetric ligands and the one pypz asymmetric ligand involved in this complex. Thus, one set of features is associated with the bpy ligand and exhibits frequencies and relative intensities which are very similar to those observed for $Ru(bpy)_3^{2+}$. As has been thoroughly discussed in previous work,[5a] the vibrational modes of the pypz ligand are conveniently classified into three categories. One subset is associated with the vibrations of the periphery of the pyridine fragment, while another is attributable to the periphery of the pyrazine fragment. A third subset involves motions of the C−C inter-ring and adjacent bonds. This subset of modes is observed at frequencies intermediate between the corresponding modes

(12) Danzer, G. D. Ph.D. Dissertation, Marquette University, 1992.

(13) Juris, A.; Balzani, V.; Barigelletti, F.; Campagna, S.; Belser, P.; Von Zelewsky, A. *Coord. Chem. Rev.* **1988**, *84*, 85−277.

(14) Strommen, D. P.; Mallick, P. K.; Danzer, G. D.; Lumpkin, R. S.; Kincaid, J. R. *J. Phys. Chem.* **1990**, *94*, 1357.

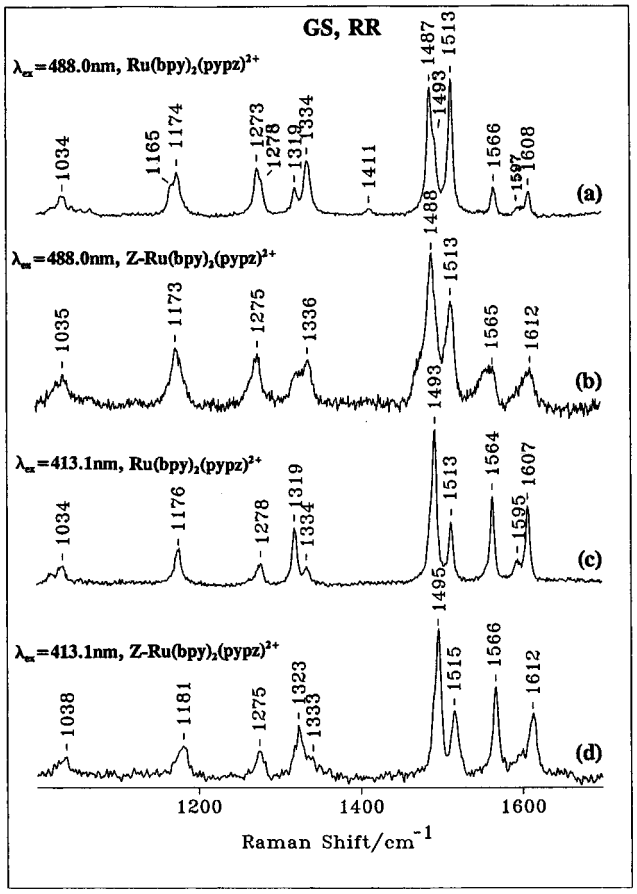

Figure 3. Resonance Raman spectra of aqueous $[Ru(bpy)_2(pypz)]Cl_2$ (1 mM) and $Z-Ru(bpy)_2(pypz)^{2+}$ (load of 1:15) suspended in DI water, acquired with 488.0 and 413.1 nm excitation, respectively (accumulation of four scans; 1 cm^{-1}/s, slit of 100 μm, 23 °C).

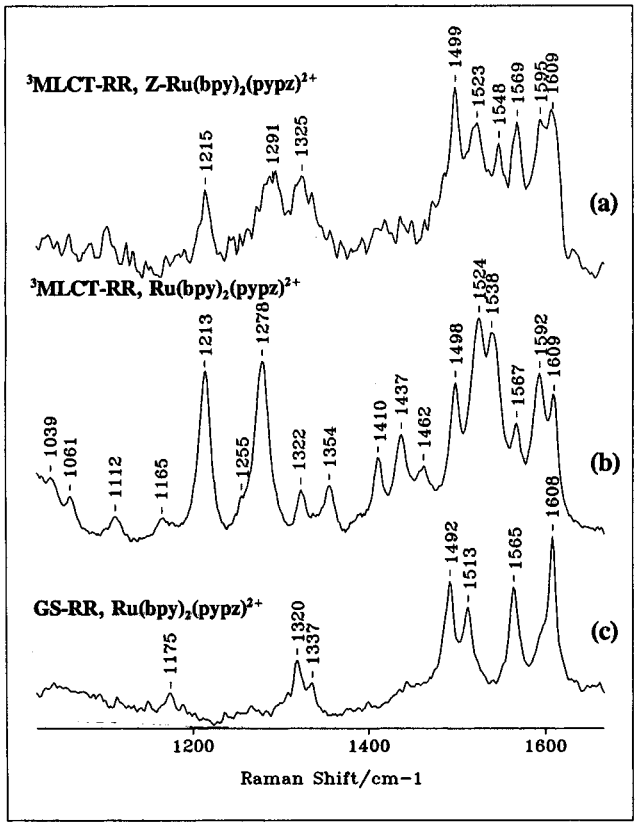

Figure 4. (a) TR^3 spectrum of the intrazeolitic $Z-Ru(bpy)_2(pypz)^{2+}$ complex (load of 1:15) acquired with 354.7 nm excitation (pulse rate 20 Hz, laser power 110 mW). (b) TR^3 spectrum of the aqueous $[Ru(bpy)_2(pypz)]Cl_2$ complex (3 mM) acquired with 354.7 nm excitation (pulse rate 20 Hz, laser power 110 mW). (c) RR spectrum of the aqueous $[Ru(bpy)_2(pypz)]Cl_2$ complex obtained with 350.9 nm excitation (500 acquisitions, exposure time 0.5 s, 20 °C).

of the bpy and bpz ligands. For example, the (mainly) $\nu(C_2-C_{2'})$ inter-ring stretch occurs at ~1320 and 1345 cm^{-1} for bpy and bpz, respectively. The corresponding mode for the pypz ligand occurs at ~1334 cm^{-1}.

Inasmuch as the low-energy side of the MLCT absorption band is presumably dominated by the Ru → pypz transition, the use of RR excitation lines (e.g., 488.0 nm) in this region are expected to selectively enhance modes associated with the pypz ligand. Conversely, excitation lines (e.g., 413.1 nm) within the high-energy side should give rise to selective enhancement of bpy modes. Clearly, the observed spectral patterns given in Figure 3 generally confirm this expected behavior.[5a] Thus, with 488.0 nm excitation, the pypz modes (e.g., those at 1334, 1487, and 1513 cm^{-1}) are selectively enhanced relative to the bpy ligand modes (e.g., those at 1319 and 1493 cm^{-1}). With 413.1 nm excitation, the enhancement patterns are reversed; i.e., the 1319 cm^{-1} mode is much stronger than the 1334 cm^{-1} mode.

As is clear from inspection of traces b and d of Figure 3, there are no substantial shifts of any vibrational modes upon incorporation of the complex within the Y-zeolite supercages. Apparently, the interaction of the peripheral N heteroatom of the complex with the zeolite framework, evidenced by the 16 nm blue shift observed in the emission spectra, is not sufficient to cause significant shift of the internal modes of the complexed pypz ligand in its ground state.

In Figure 4 are shown the TR^3 spectra of both the free complex and the zeolite-entrapped complex along with the ground state RR spectrum of the free complex obtained with 350.9 nm excitation (i.e., a frequency which closely matches that used for the TR^3 spectra). As has been thoroughly discussed previously,[5a] the TR^3 spectrum of the free complex, $Ru(bpy)_2(pypz)^{2+}$, is most reasonably interpreted in terms of selective population of a pypz-localized ^{3}MLCT excited state; i.e., the proper formulation of the excited state is $[Ru^{3+}(bpy)_2(pypz^-)]^{2+}$. Thus, no modes characteristic of a bpy^- radical anion are observed. Furthermore, within the $pypz^-$ anion, electron density is apparently polarized toward the pyrazine fragment.[5a]

The TR^3 spectrum of the zeolite-entrapped complex, $Z-Ru(bpy)_2(pypz)^{2+}$, confirms the persistence of a pypz-localized excited state (i.e., no bpy^- modes are observed) but reveals that there is some structural perturbation of the $pypz^-$ radical based on several rather significant frequency shifts (especially for the modes observed at 1538/1548 and 1278/1291 cm^{-1}) and alterations in relative intensities of bands shown in the spectra given in traces a and b.

These RR and TR^3 results are consistent with the observed absorption and emission spectral changes upon zeolite entrapment. Thus, the absorption spectra, which are diagnostic of a ground state−^{1}MLCT state transition, show no substantial changes upon zeolite entrapment, consistent with virtually identical RR spectra for the ground state in both systems. However, the 16 nm blue shift observed for the transition involving the lowest-lying ^{3}MLCT state is consistent with the TR^3 evidence for perturbation of this state (i.e., the 10−13 cm^{-1} frequency shifts).

C. Lifetime Measurements. In Figure 5a are illustrated the emission decay profiles acquired for a dilute (10^{-5} M) aqueous solution of the $[Ru(bpy)_2(pypz)]Cl_2$ complex at λ_{em} =

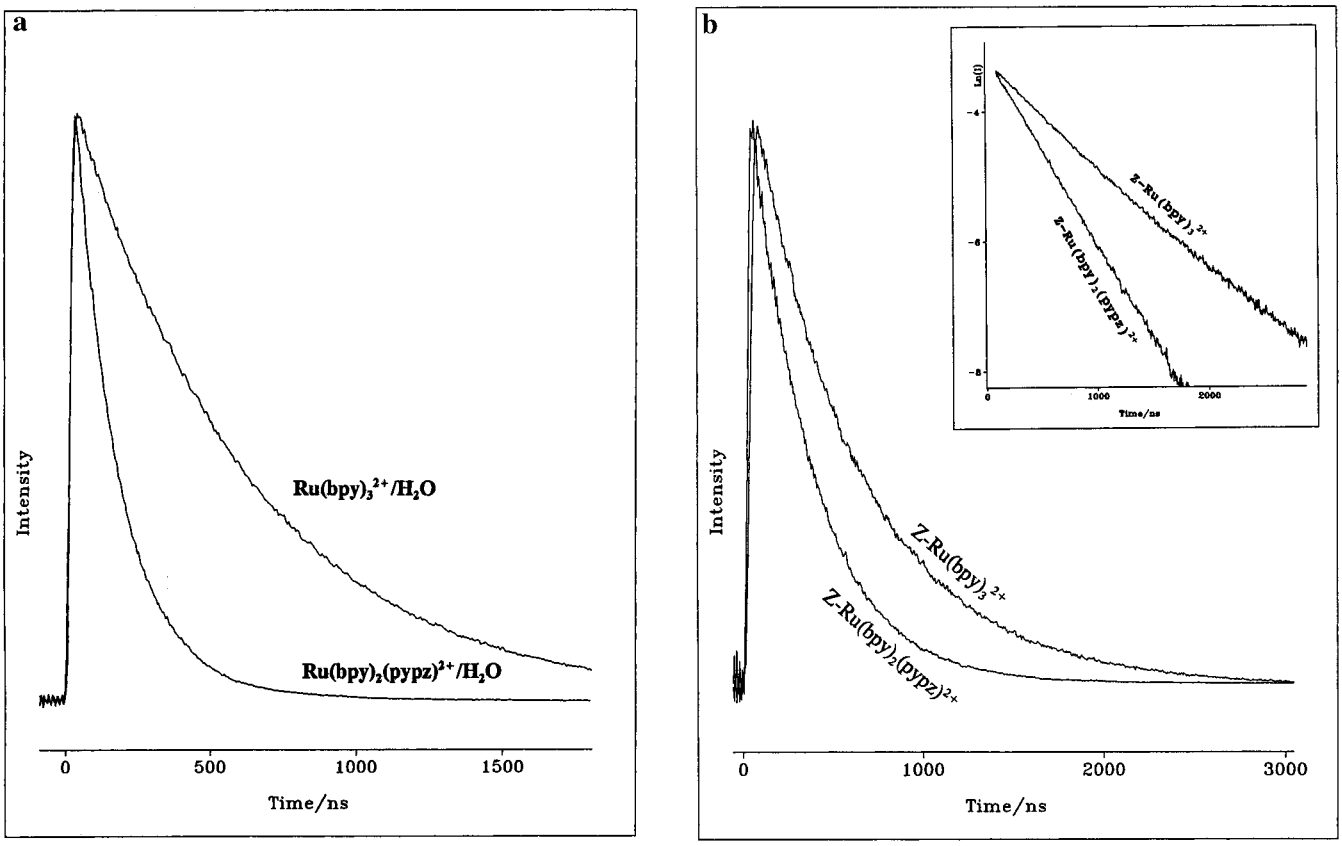

Figure 5. (a) Emission trace decay of degassed aqueous $[Ru(bpy)_3]Cl_2$ acquired at $\lambda_{em} = 610$ nm and of degassed aqueous $[Ru(bpy)_2(pypz)]Cl_2$ acquired at $\lambda_{em} = 672$ nm, with 354.7 nm excitation, at 20 °C. (b) Emission trace decay of degassed $Z-Ru(bpy)_2(pypz)^{2+}$ (load of 1:60) suspended in DI water, acquired at $\lambda_{em} = 656$ nm, and degassed aqueous $Z-Ru(bpy)_3^{2+}$ (load of 1:30), acquired at $\lambda_{em} = 618$ nm, with 354.7 nm excitation, at 20 °C. The insert shows the same experimental data for $Z-Ru(bpy)_2(pypz)^{2+}$ and $Z-Ru(bpy)_3^{2+}$, but on a logarithmic scale.

Table 1. Emission Maxima and ^{3}MLCT Excited State Lifetimes, τ_T, for Zeolite-Entrapped and Water-Diluted Polypyridine Ru^{2+} Complexes, at 297 K

	emission (nm)		τ_T (ns)		
complex	Z	H_2O	Z	H_2O	ref
$Ru(bpy)_2(pypz)^{2+}$	656	672	385	175	
$Ru(bpy)_2(bpz)^{2+}$	674	705	344	127	1b
$Ru(bpy_3^{2+}$	618	609	615	605	16b
$Ru(bpz)_3^{2+}$	598	600	1433	853	1b

672 nm and for the aqueous (10^{-5} M) $[Ru(bpy)_3]Cl_2$ complex at $\lambda_{em} = 610$ nm (with 354.7 nm excitation, at 298 K). Both of these profiles exhibit monoexponential behavior, yielding ^{3}MLCT excited-state lifetimes (τ_T) as listed in Table 1, along with data previously obtained for related complexes involving bpy and bpz ligands. Care needs to be taken in trying to directly correlate zeolite-induced emission energy shifts with changes in lifetime. Thus, shifts in emission maxima between two complexes or between the same complex in two different environments (e.g., H_2O and zeolite) are expected to follow energy gap law behavior [15] only when participation of other nonradiative pathways are unaltered. As has been pointed out by Meyer and co-workers,[15] for the class of polypyridine complexes there are, in principle, two alternative (thermally activated) nonradiative decay pathways available in addition to direct nonradiative decay from the lowest lying ^{3}MLCT state. The most efficient of these two involves thermal population of a ligand field (LF) state (also called a ^{3}dd state) which, in most complexes, lies about 3000 cm^{-1} above the ^{3}MLCT state. If this LF state lies too high in energy, then the pathway involving the other (lower lying) excited state (the so-called "4th-MLCT" state) can also make a detectable contribution to the overall decay rate of the excited-state population.[15c,16a] Documentation of participation of these two thermally activated pathways and determination of the relevant energy gaps and rate constants can be obtained by carefully fitting lifetime data, acquired over a range of temperatures, to the expression

$$1/\tau_T = k_1 + k_{LF}\exp(-\Delta E_{LF}/k_BT) + k_{4th}\exp(-\Delta E_{4th}/k_BT)$$

where τ_T = lifetime at temperature T, $k_1 = k_r + k_{nr}$, radiative and nonradiative decay rate constants, k_{LF} = preexponential factor corresponding to the thermal population rate constant of the ^{3}dd state, ΔE_{LF} = energy gap between ^{3}MLCT and LF states, k_{4th} = preexponential factor corresponding to the thermal population of 4th-MLCT electronic excited state, ΔE_{4th} = energy gap between ^{3}MLCT and 4th-MLCT electronic excited states, and k_B = Boltzmann's constant.

In most cases, the thermal sensitivity is dominated by participation of the LF state, masking minor contributions from the 4s state, and the plot of τ_T vs T can be adequately fit using an expression involving only the LF state thermal term. This

(15) (a) Allen, G. H.; White, R. P.; Rillema, D. P.; Meyer, T. *J. J. Am. Chem. Soc.* **1984**, *106*, 2613. (b) Kober, E. M.; Meyer, T. J. *Inorg. Chem.* **1984**, *23*, 3877. (c) Lumpkin, R. S.; Kober, E. M.; Worl, L. A.; Murtaza, Z.; Meyer, T. J. *J. Phys. Chem.* **1990**, *94*, 239. (d) Rillema, D. P.; Blanton, C. B.; Shaver, R. J.; Jackman, D. C.; Boldaji, M.; Bundy, S.; Worl, L. A.; Meyer, T. J. *Inorg. Chem.* **1992**, *31*, 1600.

(16) (a) Sykora, M.; Kincaid, J. R. *Inorg. Chem.* **1995**, *34*, 5852−5855. (b) Sikora, M.; Kincaid, J. K.; Dutta, P. K.; Castagnola, N. B. *J. Phys. Chem.*, submitted.

Table 2. Photopysical Parameters for Selected Ru^{2+} Polypyridine Complexes Obtained from Temperature-Dependent Lifetime Measurements

complex	k_1 (s^{-1})	k_{4th} (s^{-1})	ΔE_{4th} (cm^{-1})	k_{LF} (s^{-1})	ΔE_{LF} (cm^{-1})	ref
$Z-Ru(bpy)_2(pypz)^{2+}$	8.21×10^5	6.04×10^7	703			
$Ru(bpy)_2(pypz)^{2+}$/PC	1.01×10^6	1.95×10^7	764			
$Z-Ru(bpy)_2(bpz)^{2+}$	5.4×10^5	1.9×10^8	894			1b
$Ru(bpy)_2(bpz)^{2+}$/PC	2.1×10^6	$(3-9) \times 10^7$	800			15a
$Z-Ru(bpy)_3^{2+}$	3.8×10^5	1.1×10^8	890			1b
$Ru(bpy)_3^{2+}$/PC	6.1×10^5			4.0×10^{12}	3275	1c
$Z-Ru(bpz)_3^{2+}$	4.1×10^5	1.1×10^5	765			1b
$Ru(bpz)_3^{2+}$/PC	3.3×10^5			8.0×10^{12}	3325	1c

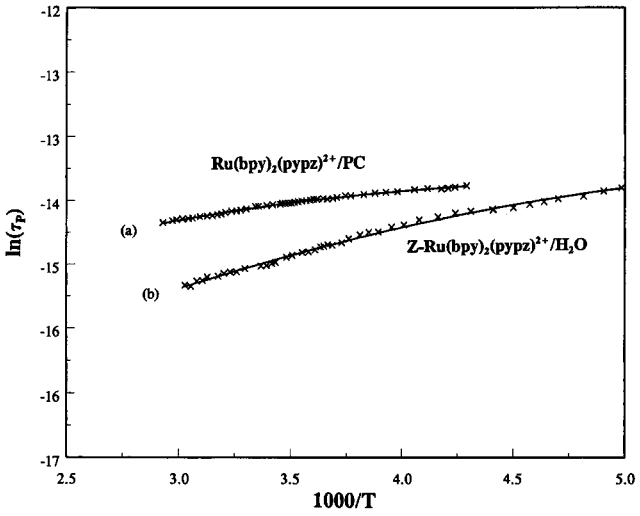

Figure 6. Temperature-dependent lifetime data obtained for (a) $[Ru(bpy)_2(pypz)]Cl_2$ dissolved in PC (10^{-5} M) and (b) the intrazeolitic $Z-Ru(bpy)_2(pypz)^{2+}$ complex (load of 1:60) suspended in DI water. The experimental points are marked by "x". The solid line represents a monoexponential fit obtained using the following expression: $1/\tau_T = k_1 + k_{4th} \exp(-\Delta E_{4th}/k_B T)$.

is the case for both $Ru(bpy)_3^{2+}$ and $Ru(bpz)_3^{2+}$ in free solution.[15a] In other cases, such as $Ru(bpy)_2(bpz)^{2+}$, the LF state is sufficiently high above the lowest lying ^{3}MLCT state that it does not substantially contribute to the decay. In these cases, a weak temperature dependence is observed resulting from participation of the "4th-MLCT" state and quite different values of ΔE and preexponential factors are obtained. As was shown recently,[16a] in certain cases the ΔE gaps are such that the τ_T vs T plots cannot be adequately fit without including contributions from both thermally activated pathways.

As has be clearly documented in earlier work,[1b,c] the major effect of zeolite entrapment of ruthenium polypyridine complexes is to destabilize the LF state to such an extent that its contribution to the overall decay rate is small or negligible. Thus, the ^{3}MLCT state lifetimes of certain complexes which have a very low-lying LF state can be dramatically increased by entrapment within the Y-zeolite supercages.[15c]

In this work, two samples of the $Z-Ru(bpy)_2(pypz)^{2+}$ complex were studied. The first sample was with a load of 1 complex per 60 supercages (1:60) and the second one with a load of 1 complex per 15 supercages (1:15). The emission decay of the low-loaded sample (1:60) was satisfactorily fit by a monoexponential expression as shown in Figure 5b. This indicated only one emitting component at 656 nm with $\tau_T =$ 385 ns (at 297 K). However, for the higher-loaded sample (1:15) the use of a biexponential expression was necessary to obtain good fits to the experimental data. Thus, two distinct lifetime components were extracted (360 and 160 ns, at 297 K); however, the percentage of the short-component emission was 20% only. The results match those estimated for emission of intrazeolitic adjacent pairs.[16b] It is important to emphasize that the long τ_T, at the load of 1:15, was approximately the same as the value obtained for the low-loaded sample (1:60). Thus, for the temperature-dependent lifetime experiments, only the sample with the 1:60 load was used.

In the present case, $Ru(bpy)_2(pypz)^{2+}$, lifetime data were obtained over a wide range of temperatures for both the free complex (in PC) and the $Z-Ru(bpy)_2(pypz)^{2+}$ sample (suspended in water), the plots obtained being given in Figure 6. As is shown in Table 2, analysis of such data for the free complex yields parameters characteristic of "4th-MLCT state" involvement; i.e., the parameters are similar to those obtained for $Ru(bpy)_2(bpz)^{2+}$ and other complexes known to have inaccessible LF states.[1b,c,15] To the extent that the LF state for this complex is already inaccessible in free solution, it is not expected that the zeolite entrapment would have dramatic effects of the ^{3}MLCT state lifetime, in agreement with the relatively modest increase observed (175 vs 385 ns). Also, inasmuch as the ΔE gap between the lowest lying (emitting) ^{3}MLCT state and the 4th-MLCT state remains comparable upon zeolite entrapment (703 vs 764 cm^{-1}), this so-called 4th-MLCT state is apparently destabilized by the interaction with the zeolite framework to the same extent as the lowest lying ^{3}MLCT state (i.e., ~16 nm).

Concluding Remarks

The present study describes the successful preparation of a new zeolite-entrapped polypyridine complex of Ru^{2+} which should prove useful as a precursor for construction of zeolite-entrapped organized molecular assemblies.[2] Spectroscopic and photophysical characterization of the entrapped complex confirms the persistence of inherent structural and photophysical properties upon entrapment, providing evidence for only slight perturbations in the structure and stability of the lowest lying ^{3}MLCT states, a perturbation which presumably arises from a specific intermolecular interaction of the peripheral N atom of the coordinated pypz ligand with the zeolite framework.

Acknowledgment. This work was supported by the Division of Chemical Science, U.S. Department of Energy (Grant DE-FG-02-86ER13619).

IC971088T